Investigation of Interaction between Synchrotron Radiation and Thulium Nanoparticles for Human Cancer Cells, Tissues and Tumors Treatment

Alireza Heidari[1,2]
Katrina Schmitt[1]
Maria Henderson[1]
Elizabeth Besana[1]

[1]California South University, USA
[2]American International Standards Institute, USA

Abstract. In the current study, thermoplasmonic characteristics of Thulium nanoparticles with spherical, core–shell and rod shapes are investigated. In order to investigate these characteristics, interaction of synchrotron radiation emission as a function of the beam energy and Thulium nanoparticles were simulated using 3D finite element method. Firstly, absorption and extinction cross sections were calculated. Then, increases in temperature due to synchrotron radiation emission as a function of the beam energy absorption were calculated in Thulium nanoparticles by solving heat equation. The obtained results show that Thulium nanorods are more appropriate option for using in optothermal human cancer cells, tissues and tumors treatment method.

Key words*:* Thulium Nanoparticles, Scanning Electron Microscope (SEM), 3D Finite Element Method (FEM), Heat Transfer Equation, Thermoplasmonic, Thulium Nanorods, Beam Energy.

Introduction

In recent decade, metallic nanoparticles have been widely interested due to their optical characteristics and potential in cancer treatment (Heidari and Brown, 2015a: 20; Heidari and Brown, 2015b: 15-19; Heidari, 2016a-c). Resonances of surface Plasmon in these nanoparticles lead to increase in synchrotron radiation emission as a function of the beam energy scattering and absorption in related frequency (Heidari, 2016d-e). Synchrotron radiation emission as a function of the beam energy absorption and induced produced heat in nanoparticles has been considered as a side effect in plasmonic applications for a long time (Heidari, 2016f-g). Recently, scientists find that thermoplasmonic characteristic can be used for various optothermal applications in cancer, nanoflows and photonic (Heidari, 2016h-j; Andresen and Albrechtsen, 2013; Li et al., 2019; Guo, 2008; Borghi et al., 2015; Kakade et al., 2019; Hainfeld et al., 2019: 4505). In optothermal human cancer cells, tissues and tumors treatment, the descendent laser light stimulate resonance of surface Plasmon of metallic nanoparticles and as a result of this process, the absorbed energy of descendent light converse to heat in nanoparticles (Heidari, 2016h-j). The produced heat devastates tumor tissue adjacent to nanoparticles without any hurt to sound tissues (Heidari, 2016j; Brown et al., 2017; Bonvicini et al., 2015). Regarding the simplicity of ligands connection to Thulium nanoparticles for targeting cancer cells, these nanoparticles are more appropriate to use in optothermal human cancer cells, tissues and tumors treatment (Heidari, 2016j; Engels et al., 2016; Engels et al., 2018). In the current paper, thermoplasmonic characteristics of spherical, core-shell and rod Thulium nanoparticles are investigated (Fig.1).

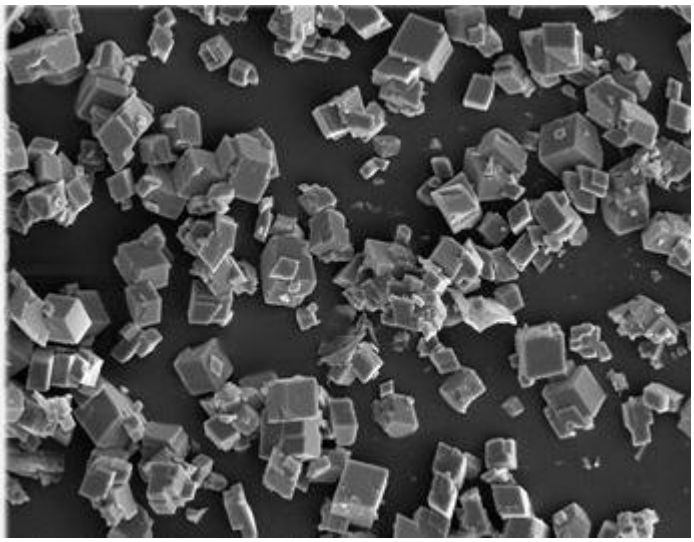

Fig. 1. Scanning Electron Microscope (SEM) image of Thulium nanoparticles with 50000x zoom.

Materials and Methods

When Thulium nanoparticles are subjected to descendent light, a part of light scattered (emission process) and the other part absorbed (non–emission process). The amount of energy dissipation in non–emission process mainly depends on material and volume of nanoparticles and it can be identified by absorption cross section. At the other hand, emission process which its characteristics are depend on volume, shape and surface characteristics of nanoparticles explains by scattering cross section. Sum of absorption and scattering processes which lead to light dissipation is called extinction cross section.

Thulium nanoparticles absorb energy of descendent light and generate some heat in the particle. The generated heat transferred to the surrounding environment and leads to increase in temperature of adjacent points to nanoparticles. Heat variations can be obtained by heat transfer equation.

To calculate the generated heat in Thulium nanoparticles, COMSOL software which works by Finite Element Method (FEM) was used. All simulations were made in 3D. Firstly, absorption and scattering cross section areas were calculated by optical module of software. Then, using heat module, temperature variations of nanoparticles and its surrounding environment were calculated by data from optical module. In all cases, Thulium nanoparticles are presented in water environment with dispersion coefficient of 1.84 and are subjected to flat wave emission with linear polarization. Intensity of descendent light is 1 $mW/\mu m^2$. Dielectric constant of Thulium is dependent on particle size.

Results and Discussion

Firstly, calculations were made for Thulium nanospheres with radius of 5, 10, 15, 20, 25, 30, 35, 40, 45 and 50 nanometers. The results show that by increase in nanoparticles size, extinction cross section area increases and maximum wavelength slightly shifts toward longer wavelengths. The maximum increase in temperature of nanospheres in surface Plasmon frequency is shown in Fig. 2.

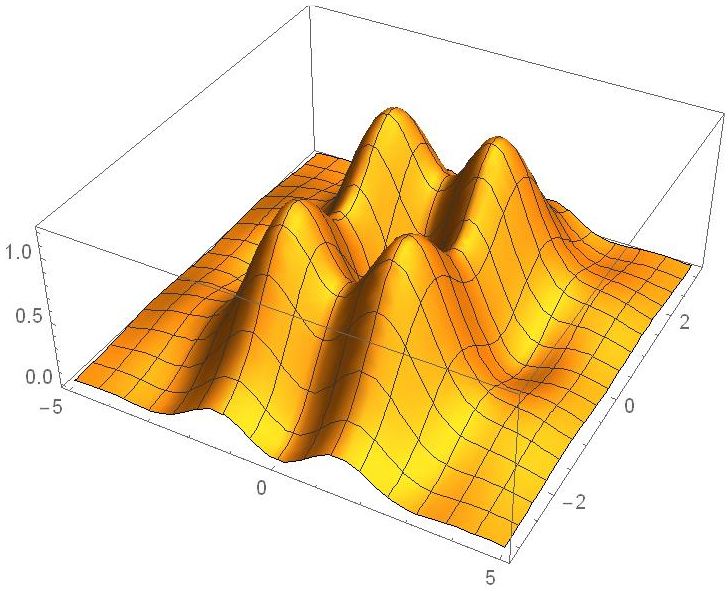

Fig. 2. Maximum increase in temperature for Thulium nanospheres.

According to the graph, it can be seen that the generated heat is increased by increase in nanoparticles size. For 100 (nm) nanoparticles (sphere with 50 (nm) radius), the maximum increase in temperature is 83 (K). When nanoparticles size reaches to 150 (nm), increase in temperature is increased in spite of increase in extinction coefficient. In order to find the reason of this fact, ratio of absorption to extinction for various nanospheres in Plasmon frequency is shown in Fig. 3.

Fig. 3 shows that increasing the size of nanospheres leads to decrease in ratio of light absorption to total energy of descendent light so that for 150 (nm) nanosphere, scattering is larger than absorption. It seems that although increase in nanoparticles size leads to more dissipation of descendent light, the dissipation is in the form of scattering and hence, it cannot be effective on heat generation.

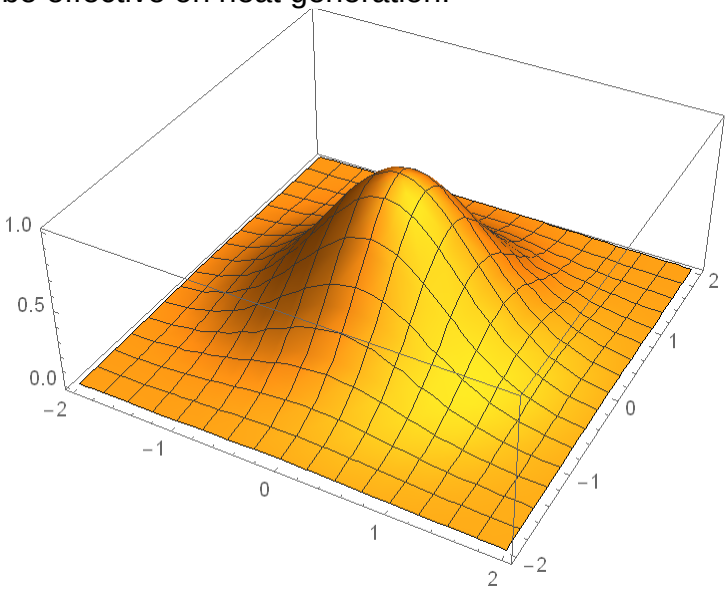

Fig. 3. Variations of absorption to extinction ratio and scattering to extinction ratio for Thulium nanospheres with various radiuses.

Heat distribution (Fig. 4) shows that temperature is uniformly distributed throughout the nanoparticles which are due to high thermal conductivity of Thulium.

In this section, core-shell structure of Thulium and silica is chosen. The core of a nanosphere with 45 (nm) radius and silica layer thickness of 5, 10, 15, 20, 25, 30, 35, 40, 45 and 50 nanometers are considered. The results show that increase in silica thickness leads to increase in extinction coefficient and shift in Plasmon wavelength of nanoparticles, to some extent.

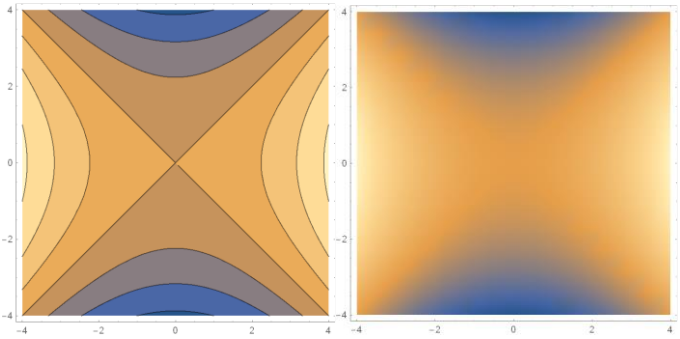

Fig. 4. Maximum increase in temperature for spherical nanoparticles with radius of 45 (nm) at Plasmon wavelength of 685 (nm).

According to Fig. 5, silica shell causes to considerable increase in temperature of Thulium nanoparticles but by more increase in silica thickness, its effects are decreased. Heat distribution (Fig. 6) shows that temperature is uniformly distributed throughout metallic core as well as silica shell. However, silica temperature is considerably lower than core temperature due to its lower thermal conductivity. In fact, silica layer prohibits heat transfer from metal to the surrounding aqueous environment due to low thermal conductivity and hence, temperature of nanoparticles has more increase in temperature. Increasing the thickness of silica shell leads to increase in its thermal conductivity and hence, leads to attenuate in increase in nanoparticles temperature.

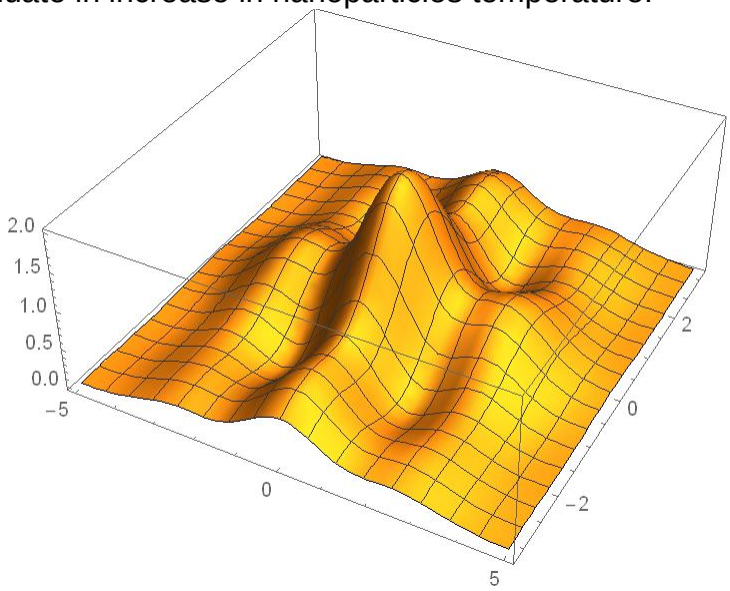

Fig. 6. Maximum increase in temperature for core–shell Thulium nanospheres with various thicknesses of silica shell.

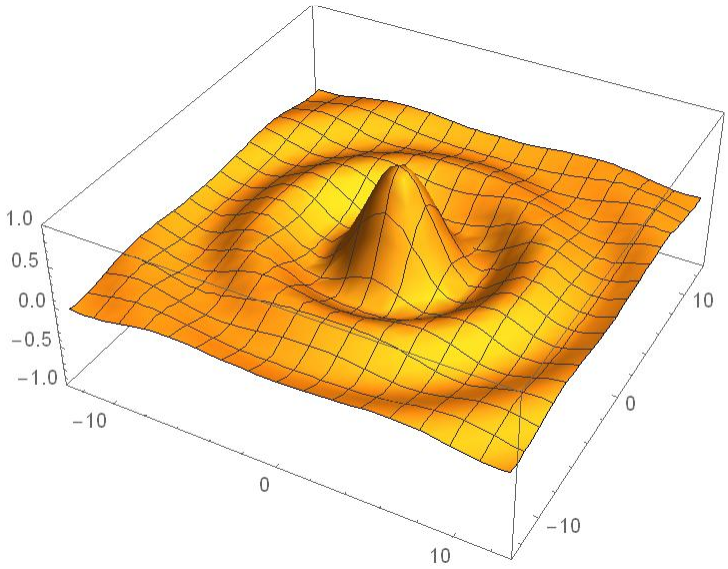

Fig. 6. Maximum increase in temperature for core–shell nanoparticles with radius of 45 (nm) and silica thickness of 10 (nm) at Plasmon wavelength of 701 (nm).

Figure 7 is drawn. This graph shows that variation of nanorod dimension ratio leads to considerable shift in Plasmon wavelength. This fact allows regulating the Plasmon frequency to place in near IR zone. Light absorption by body tissues is lower in this zone of spectrum and hence, nanorods are more appropriate for optothermal human cancer cells, tissues and tumors treatment methods.

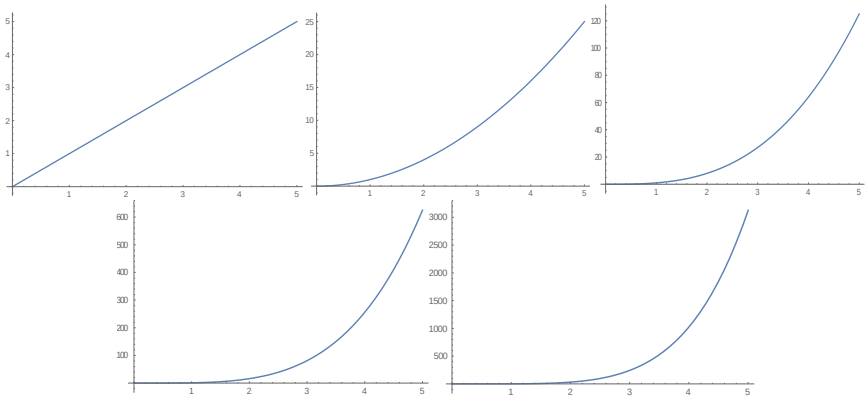

Fig. 7. Extinction cross section area for Thulium nanorods with effective radius of 45 (nm) and various dimension ratios.

Variations of temperature in Thulium nanorods with two effective radius and various dimension ratios are shown in Fig. 8. By increase in length (a) to radius (b) of nanorod, temperature is increased.

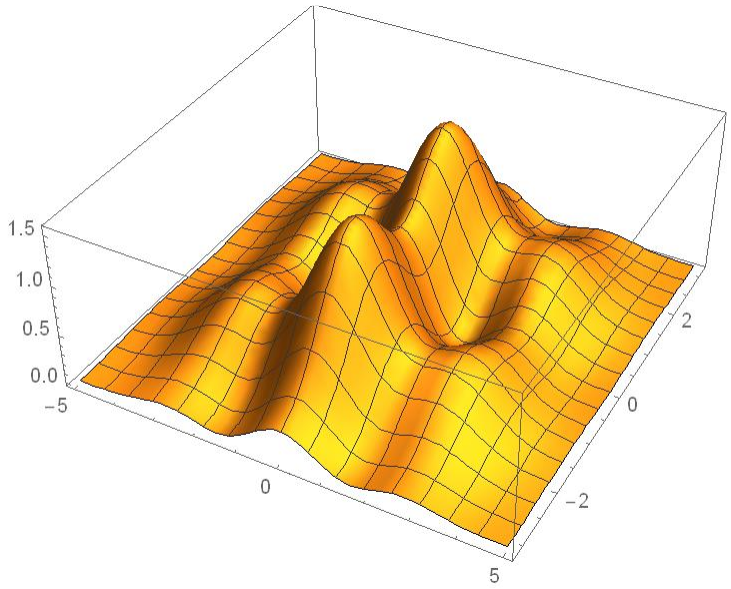

Fig. 8. Maximum increase in temperature for nanorods with effective radius of 20 and 45 (nm) and various dimension ratios.

Conclusion

The calculations showed that in Thulium nanoparticles, light absorption in Plasmon frequency causes to increase in temperature of the surrounding environment of nanoparticles. In addition, it showed that adding a thin silica layer around the Thulium nanospheres increases their temperatures. Calculations of nanorods showed that due to ability for shifting surface Plasmon frequency toward longer wavelength as well as more increase in temperature, this nanostructure is more appropriate for medical applications such as optothermal human cancer cells, tissues and tumors treatments.

Acknowledgements

Authors are supported by an American International Standards Institute (AISI) Future Fellowship Grant FT12010093734713. We acknowledge Ms. Isabelle Villena for instrumental support and Dr. Michael N. Cocchi for constructing graphical abstract figures. We gratefully acknowledge Prof. Dr. Christopher Brown for proof reading the manuscript. Synchrotron beam time was awarded by the National Synchrotron Light Source (NSLS–II) under the merit–based proposal scheme.

References

Andresen, T.L., Albrechtsen, M. (2013). Nanoparticle-guided radiotherapy. Google Patents. US 2013/0204121 A1. Available at: https://patentimages.storage.googleapis.com/66/62/7d/ecffca1facfe7a/US20130204121A1.pdf

Bonvicini, S. (2015). Colloidal Lanthanide-Based Nanoparticles: From Single Nanoparticle Analysis to New Applications in Lasing and Cancer Therapy. Colloidal Lanthanide-Based Nanoparticles: From Single Nanoparticle Analysis to New Applications in Lasing and Cancer Therapy. Available at: http://hdl.handle.net/1828/6982

Borghi, I., Levy, L., Pottier, A. (2015). Inorganic nanoparticles compositions in combination with ionizing radiations for treating cancer. Google Patents. US 2015/0374818A1. Available at: https://patentimages.storage.googleapis.com/e5/6b/fe/15bd5c91882915/US20150374818A1.pdf

Brown, R., Corde, S., Oktaria, S., Konstantinov, K., Rosenfeld, K., Lerch, M., Tehei, M. (2017). Nanostructures, concentrations and energies: an ideal equation to extend therapeutic efficiency on radioresistant 9L tumor cells using Ta2O5 ceramic nanostructured particles. Biomed. Phys. Eng. Express, 3, 015018. Available at: https://iopscience.iop.org/article/10.1088/2057-1976/aa56f2/pdf

Engels, E., Lerch, M., Tehei, M., Konstantinov, K., Guatelli, S., Rosenfeld, A., Corde, S. (2016). Synchrotron activation radiotherapy: Effects of dose-rate and energy spectra to tantalum oxide nanoparticles selective tumour cell radiosensitization enhancement. Journal of Physics: Conference Series, 777, 012011. Available at: https://iopscience.iop.org/article/10.1088/1742-6596/777/1/012011/pdf

Engels, E., Westlake, M., Li, N., Vogel, S., Gobert, Q., Thorpe, N., Rosenfeld, A., Lerch, M., Corde, S., Tehei, M. (2018). Thulium Oxide Nanoparticles: A new candidate for image-guided radiotherapy. Biomedical Physics & Engineering Express, 4(4), 044001.

Guo, T. (2008). Nanoparticle radiosensitizers. Google Patents. US 2008/0003183 A1. Available at: https://patentimages.storage.googleapis.com/e7/fa/3f/6c599866fe6797/US20080003183A1.pdf

Hainfeld, J.F., Ridwan, S.M., Stanishevskiy, Y. (2019). Iodine nanoparticles enhance radiotherapy of intracerebral human glioma in mice and increase efficacy of chemotherapy. Sci Rep, 9, 4505.

Heidari, A. (2016d). A Bio–Spectroscopic Study of DNA Density and Color Role as Determining Factor for Absorbed Irradiation in Cancer Cells. Adv Cancer Prev, 1, e102.

Heidari, A. (2016a). An Experimental Biospectroscopic Study on Seminal Plasma in Determination of Semen Quality for Evaluation of Male Infertility", Int J Adv Technol, 7, e007.

Heidari, A. (2016b). Extraction and Preconcentration of N–Tolyl–Sulfonyl–Phosphoramid–Saeure–Dichlorid as an Anti–Cancer Drug from Plants: A Pharmacognosy Study. J Pharmacogn Nat Prod, 2, e103.

Heidari, A. (2016c). A Thermodynamic Study on Hydration and Dehydration of DNA and RNA−Amphiphile Complexes", J Bioeng Biomed Sci S, 006.

Heidari, A. (2016e). Manufacturing Process of Solar Cells Using Cadmium Oxide (CdO) and Rhodium (III) Oxide (Rh_2O_3) Nanoparticles. J Biotechnol Biomater, 6, 125.

Heidari, A. (2016f). A Novel Experimental and Computational Approach to Photobiosimulation of Telomeric DNA/RNA: A Biospectroscopic and Photobiological Study. J Res Development, 4, 144.

Heidari, A. (2016g). Biochemical and Pharmacodynamical Study of Microporous Molecularly Imprinted Polymer Selective for Vancomycin, Teicoplanin, Oritavancin, Telavancin and Dalbavancin Binding", Biochem Physiol, 5, e146.

Heidari, A. (2016h). Biomedical Study of Cancer Cells DNA Therapy Using Laser Irradiations at Presence of Intelligent Nanoparticles", J Biomedical Sci. 5: 2.

Heidari, A. (2016i). Measurement the Amount of Vitamin D2 (Ergocalciferol), Vitamin D3 (Cholecalciferol) and Absorbable Calcium (Ca^{2+}), Iron (II) (Fe^{2+}), Magnesium (Mg^{2+}), Phosphate (PO^{4-}) and Zinc (Zn^{2+}) in Apricot Using High–Performance Liquid Chromatography (HPLC) and Spectroscopic Techniques. J Biom Biostat, 7, 292.

Heidari, A. (2016j). Spectroscopy and Quantum Mechanics of the Helium Dimer (He^{2+}), Neon Dimer (Ne^{2+}), Argon Dimer (Ar^{2+}), Krypton Dimer (Kr^{2+}), Xenon Dimer (Xe^{2+}), Radon Dimer(Rn^{2+}) and Ununoctium Dimer (Uuo^{2+}) Molecular Cations", Chem Sci J, 7, e112.

Heidari, A., Brown, C. (2015a). Study of Composition and Morphology of Cadmium Oxide (CdO) Nanoparticles for Eliminating Cancer Cells. J Nanomed Res., 2(5), 20.

Heidari, A., Brown, C. (2015b). Study of Surface Morphological, Phytochemical and Structural Characteristics of Rhodium (III) Oxide (Rh_2O_3) Nanoparticles. International Journal of Pharmacology, Phytochemistry and Ethnomedicine, 1(1), 15-19.

Kakade, N.R., Kumar, R., Sharma, S.D., Datta, D. (2019). Equivalence of silver and gold nanoparticles for dose enhancement in nanoparticle-aided brachytherapy. Biomedical Physics & Engineering Express, 5(5), 055015.

Li, N., Engels E., Davis, J.A., Dipuglia, A., Vogel, S., Valceski, M., Rosenfeld, A.B., Lerch, M.L.F., Corde, S., Tehei, M. (2019). Polo-like kinase 1 inhibitor BI6727 sensitizes 9L gliosarcoma cells to ionizing irradiation. Biomedical Physics&Engineering Express, 5(6), 067003.